

PAPER

Promising molybdenum trioxide films for optically detectable gas sensor and solar cell applications

To cite this article: H M Ali *et al* 2019 *Mater. Res. Express* **6** 126451

View the [article online](#) for updates and enhancements.



IOP | ebooksTM

Bringing you innovative digital publishing with leading voices to create your essential collection of books in STEM research.

Start exploring the **collection** - **download the first chapter of every title for free.**

Materials Research Express



PAPER

Promising molybdenum trioxide films for optically detectable gas sensor and solar cell applications

H M Ali¹, E Kh Shokr¹, Sh A Elkot¹ and W S Mohamed^{1,2} 

¹ Physics Department, Faculty of Science, Sohag University, 82524 Sohag, Egypt

² Physics Department, College of Science, Jouf University, Al-Jouf, Sakaka, P.O. Box 2014, Saudi Arabia

E-mail: wael-saad@science.sohag.edu.e.g

Keywords: MoO_{3-x} thin films, thermal evaporation, x-ray diffraction, scanning electron microscope, chlorine gas

Abstract

Sub-stoichiometric molybdenum trioxide (MoO_{3-x}) thin films were grown by thermal evaporation techniques on glass, single crystal silicon Si and Fluorine doped Tin Oxide (FTO) glass substrates with different thicknesses. It was found that, Oxygen vacancies play an important role on properties of MoO_{3-x} films. The structural properties of these films were analyzed by means of x-ray diffraction, energy dispersive analysis of x-ray, scanning electron microscopy. The film surface uniformity and smoothness with thickness was tested using the surface roughness measurement for MoO_{3-x} films grown on glass and FTO. The optical properties of all presented films were investigated using UV–vis–near-infrared (NIR) spectrophotometer. Optical transmittance and reflection of MoO_{3-x} film were measured in the wavelength range from 200 to 2500 nm. MoO_{3-x} film with 500 nm thick was tested optically for gas sensor applications. The effect of chlorine exposure on the optical transmittance of MoO_{3-x} film with 500 nm thick deposited on glass was studied. Transmittance degradation as increasing the period of exposure was observed, indicating to the high sensitivity of MoO_{3-x} to chlorine gas. The electrical resistivity and Seebeck coefficient of MoO_{3-x} film with 500 nm thick were measured. Low resistivity ($\sim 10^{-3} \Omega \cdot \text{cm}$) and high transmittance ($\sim 78\%$) in the visible spectrum of the film of 100 nm thick deposited on FTO coated glass substrate recommended it to be promising as transparent conductive electrode for solar cell.

1. Introduction

Transition metal oxide materials with relatively high oxygen index such as MoO₃, WO₃ and V₂O₅ are n or p-type semiconductors depending on their preparation conditions [1–3]. Molybdenum trioxide (MoO₃) is one of the most important transition metal oxide materials due to its high stability [4]. MoO_{3-x} materials are widely utilized in numerous industrial applications due to their remarkable structural, optical and electrical properties [2, 4]. They can be used as catalyst or gas sensor materials [5–7], electrodes in lithium batteries [8] transparent contacts for organic photovoltaics or organic light-emitting diodes [9–11] and other optoelectronic devices [12–17].

A variety of methods have been reported for the preparation of MoO₃ thin films such as flash evaporation [4], vapor transport method [9], electron beam evaporation [10], and chemical vapor transport (CVT). [11, 18] and spray pyrolysis [7].

In this work, the thermal evaporation is selected to prepare MoO₃ thin films because of its careful control on the film thickness [4]. Moreover, the vacuum evaporated MoO₃ thin films may become sub-stoichiometric oxide (MoO_{3-x}) films [19], due to the process of oxygen deficiency that occurred during the thermal evaporation of MoO₃.

Generally, Oxygen deficiency plays an important role in the optical and electrical properties of transition metal oxide materials. The process of oxygen deficient (MoO_{3-x}) is leading to the formation of energy states within the forbidden optical band gap of the growing film by the extra Mo metallic atoms. Nadkarni and

Simmons [20] studied the electrical properties of MoO_3 and found out that there is a donor band between the conduction band and the valence band that formed due to oxygen deficient. The excess metal atoms work as doping centers and cause the n-type doping in MoO_3 thin films [5, 21]. The presence of oxygen deficiency encourages testing the growing films for gas sensor application, whereas, the sensing mechanism is based on the surface reaction of semiconducting oxide, so gases can be chemisorbed in air at the surface of the material [22].

Besides that, MoO_{3-x} thin films have characterized by chromogenic properties; Chromogenic is referred to as the ability of a material to change its optical transmittance and/or reflectance when exposed to specific external agents [23, 24]. There are different types of chromogenic effects, Thermochromism, photochromisms, and electrochromisms [24, 25]. Photochromisms can be defined as the optical changes upon exposure of a material to electromagnetic radiation. The effect of chlorine gas on the optical properties of the as deposited MoO_{3-x} thin films on glass and FTO was examined as an unconventional way for Chromogenic and examination of MoO_{3-x} thin films as a sensor towards chlorine gas.

Because of high toxicity and respiratory irritant of chlorine vapor [26], in this work, MoO_{3-x} films will be tested for using as a chlorine detection sensor. The choice of optical method is due to their straight forward, high sensitivity, high Selectivity, high stability, high resistivity to electromagnetic noise, compatibility with optical fibers, and the ability of multi-gas detection [26, 27]. The major objective of this study was to investigate the effects of the film thickness and type of substrate on the structural, optical and electrical properties of MoO_{3-x} films for various applications.

2. Experimental details

2.1. Deposition technique

MoO_3 thin film with different thicknesses (100, 200, 300, 500, 650 nm) have been deposited by thermal evaporation technique from a single source using a coating unit (Auto 306, 2014).

MoO_3 powder provided by Aldrich with 99.999% purity was compressed under pressure and placed in a molybdenum boat (melting point 2620 °C). The compressed tablet MoO_3 was used to prepare MoO_3 thin films on ultrasonically cleaned microscopic glass, single crystal silicon Si and fluorine doped tin oxide (FTO) coated glass. Substrates were cleaned rinsing by means of heated ultrasonic cleaner instrument (VGT-1613 QTD) provided with digital timer of capacity 2000 ml using both acetone and distilled water. Before deposition the chamber was evacuated to base vacuum of 4×10^{-4} mbar and the vacuum in end of deposition process was 3.63×10^{-5} mbar. The film thickness and the deposition rate were monitoring by means of a digital film thickness monitor model INFICON (SQM-160). The deposition rate was in the range from 1 to 3 Å sec^{-1} .

2.2. Investigation techniques

X-ray diffraction (XRD) examination was used for examining the crystallographic structure of the as deposited films on glass, and FTO substrates, and also for fluorine doped tin oxide (FTO) coated glass substrate before depositing the film. In this work the (XRD) examination have been carried out using x-ray diffractometer type Philips (model PW1710) with Cu as target and Ni as filter, $\lambda = 1.541838$ Å. The x-ray diffractometer work at 40 kV and 30 mA with a scanning speed 2°min^{-1} . The diffraction scan was in the range (2θ) from 10 to 100° . The surface topography and the compositional contents of some deposited MoO_3 thin films on glass and FTO (thickness 200 and 500) have been checked by field-emission scanning electron microscopy (FE-SEM) using a JSM-6100 microscope with an acceleration voltage of 30 kV. The chemical composition of the films was also analyzed using energy dispersive analysis of x-ray (EDAX) unit attached with the FE-SEM (EDS unit, HNU-5000). Very thin layer of gold ~10 nm thick has been deposited over the samples before examination. Surface roughness was measured for the as deposited films on glass and FTO using Talysurf 50 profilometer, where, a thin prop was placed to move vertically on the film surface for a distance equals to 5 nm by a step of 5×10^{-4} nm. During that, the system records all horizontal movements of the prop giving information about the degree of the deposited film surface roughness.

The optical properties (transmission T and reflectance R) were measured for as deposited films on glass and FTO at room temperature using a computer-programmable Jasco V570 double beam spectrophotometer. The wavelength range was from 200 to 2500 nm at normal incidence with a scan speed of 400 nm min^{-1} . For measuring the optical reflectivity of the films, an additional attachment model ISN-470 was used. The measured T and R values were used to determine several optical constants of the deposited MoO_{3-x} films, such as the absorption coefficient (α), the optical band gap energy E_g , hence Tauc's formula [28] was used to determine the optical band gap (E_g) of the deposited films.

MoO_{3-x} films with 500 nm thick were tested optically for chlorine gas sensor applications. The effect of chlorine exposure on the optical transmittance of MoO_{3-x} film with 500 nm thick deposited on glass and FTO coated glass substrates was studied. For that, the films were introduced into a glass chamber under variable

chlorine gas concentrations (3.3, 6.6, 9.9, 13.2, 16.5, 19.8, 23.1 and 29.7%) for fixed time period (10 min). Besides, the films were exposed to fixed concentration of chlorine (10%) for different periods of time (5, 10, 20, 40, 80, and 107 min). For testing the reversibility behavior, the films were measured again after 16 h from the last exposure to chlorine.

Electrical resistivity, ρ , was measured for MoO_{3-x} thin film with 500 nm thick deposited on glass and FTO coated glass substrates in the temperature range from 27 to 300 °C. Two-point probe technique was used to measure resistivity of the films. Silver electrodes were deposited on the film, leaving an uncoated trip (0.2 cm) in the middle of the film. The resistance of the sample was recorded by a digital ohmmeter. For more understanding the conducting behavior and determining the type of carriers; Seebeck coefficient was measured for MoO_{3-x} film with 500 nm thick, deposited on glass, and calculated using the following equation.

$$S = \Delta V / \Delta T \quad (1)$$

where, S is Seebeck coefficient which is the value of the developed electromotive force between the two ends of the thin film when the temperature difference ΔT between them equals to one degree. The developed Seebeck voltage of the sample was recorded by micro voltmeter and the temperature of the specimen was recorded by means of thermal contact chromel-alumel thermocouple with the specimen surface.

Electrical resistivity (ρ) of MoO_{3-x} thin films deposited on FTO were measured at the room temperature to calculate the figure of Merit for these films to determine the best thickness which can be used as a high transparent conductive electrode for solar devices.

3. Results and discussion

Figure 1 show the x-ray diffraction (XRD) patterns of the as-deposited molybdenum oxide thin films on glass and FTO coated glass substrates with thickness of 500 and 650 nm. For deposited films on glass, it's clear from figure 1(a) that the films have amorphous structure which may be resulted from the interstitial or substitutional locations. The x-ray diffraction patterns of MoO_{3-x} deposited on FTO substrate were presented in figure 1(b). It is observed that films contain diffraction peaks around 26.87°, 33.96°, 38.05°, 52.01°, 55.02°, 61.88°, 65.96° and 72.2°. These peaks cannot be indexed to any Mo or Molybdenum oxide phases; however they can be indexed to FTO coated glass substrate with cassiterite structure (JCPDS No.41-1445) confirming the amorphous nature of MoO_{3-x} films. This finding is in agreement with the previously reported 'Structural and optical properties of electrodeposited molybdenum oxide thin films' [29]. This amorphinity may be arisen due to the dislocations and/or point defects within the deposited films, leading to the complex structure of the energy states within the films [30]. To corroborate these results, another group of MoO_{3-x} films were deposited on Au coated FTO substrates to be $\text{MoO}_{3-x}/\text{Au}/\text{FTO}$. It was found also that, the diffraction peaks are correlated to Au and FTO; and there are no diffraction peaks were observed for MoO_{3-x} , see figure 1(c).

Figure 2 depicts the SEM micrographs for as deposited MoO_{3-x} thin films with 200 and 500 nm thick deposited on glass and FTO coated glass. As observed by figure 2, the film has a compact and dense homogenous surface. The MO films show some spherical grains with size lying in 100–200 nm domains. The orientation of these grains are randomly, some whole grains do not share a common border and so are surrounded by empty spaces. Besides, the nano spheres as well as the clusters of spheres with typically shape, in figures 2(c), (d) for the MoO_{3-x} films deposited on FTO coated glass substrates, can be observed.

The chemical composition analysis of the as deposited samples on Si substrate using energy dispersive analysis of x-ray (EDAX) is presented in figure 3 for MoO_{3-x} film of 300 nm thick as an example. EDAX analyses for all MoO_{3-x} films deposited on single crystal Si substrates indicate that, films are composed of impurity-free constituents (i.e., Mo, and O only). From Edax data, O/Mo at% ratio is about 2.3, so the formula of MoO_{3-x} film is $\text{MoO}_{2.3}$, indicating the presence of excess Mo and Oxygen deficiency $x \sim 0.7$. These metallic Mo atom vacancies in such film act as donor centers, this makes the growing films to be used as a transparent contact for organic photovoltaic or organic light-emitting diodes and promising to be used as a catalyst or sensor material [2, 31, 32].

In order to test the film surface uniformity and smoothness with thickness, surface roughness of as deposited MoO_{3-x} films on glass and FTO with different thicknesses has been measured using Talysurf 50 profilometer. The Arithmetical mean roughness (R_a μm) values are obtained from the mean height of peaks and valleys on the surface and presented in figure 4. As expected by the increment of the deposited film thickness, (R_a) values generally decreases for both films deposited on glass and FTO coated glass. It is known that the formation of thin film passes through the following different stages [33]; nucleation stage, during which the reached atoms to the substrate surface start to form small separated nuclei. These nuclei are statistically distributed over the substrate surface. In that stage of very small thickness, the film surface is highly rough. By depositing more particles on the substrate surface the nucleation growth process starts and small islands will be formed by reaching more particles to the substrate. These islands start to be coalescence to form connected network containing empty

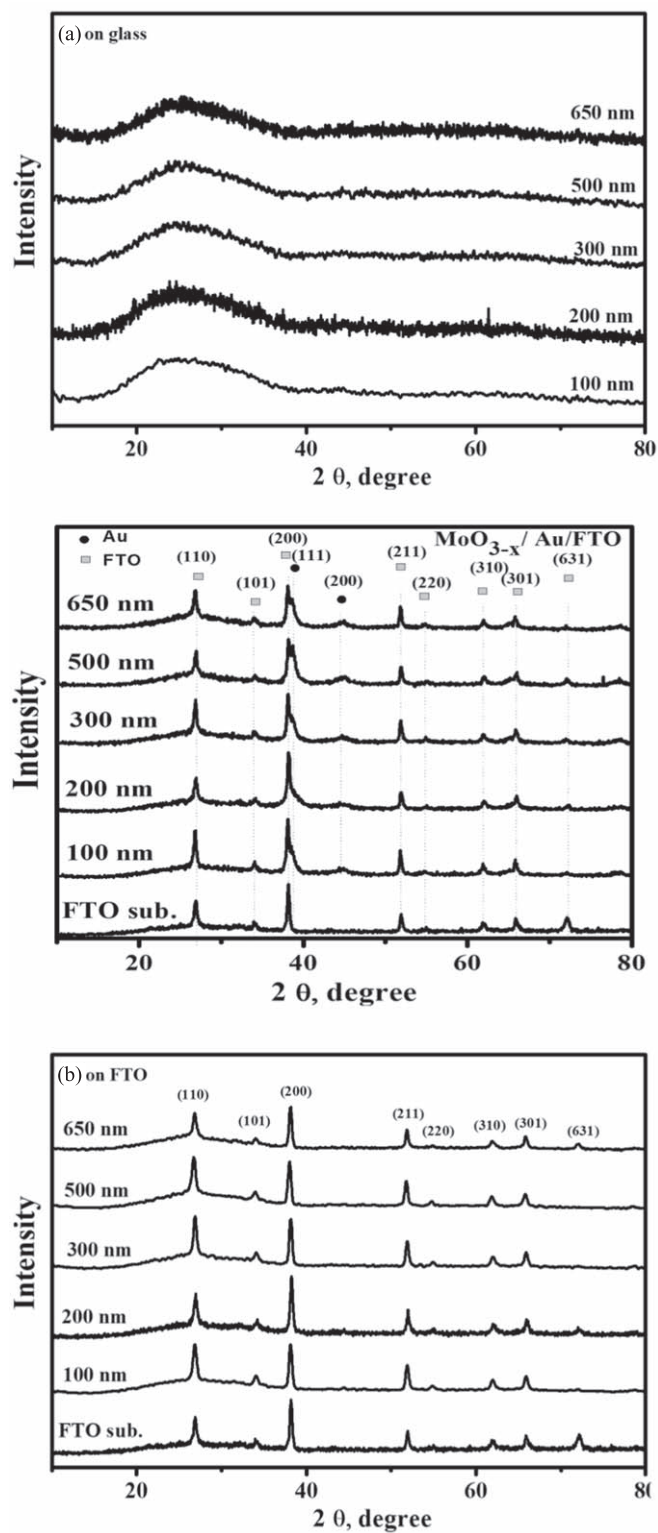


Figure 1. X-ray diffractograms of MoO_{3-x} thin films deposited on (a) glass, (b) FTO and Au/FTO substrates.

channels. These channels are filled with atoms and particles by reaching more atoms to the substrate i.e. by increasing the deposited film thickness. So, it can be concluded that, by increasing the thickness of the deposited films, the roughness of the film surface reduces. The lowest roughness (i.e. the highest film uniformity and smoothness) may be achieved at a thickness value dependent on different factors such as the deposited materials, type of substrate and deposition conditions.

As depicted in figure 4 R_a values for the as deposited MoO_{3-x} thin film on glass and FTO are generally decreases by increasing the film thickness. Values of R_a for the films deposited on glass are higher than those for

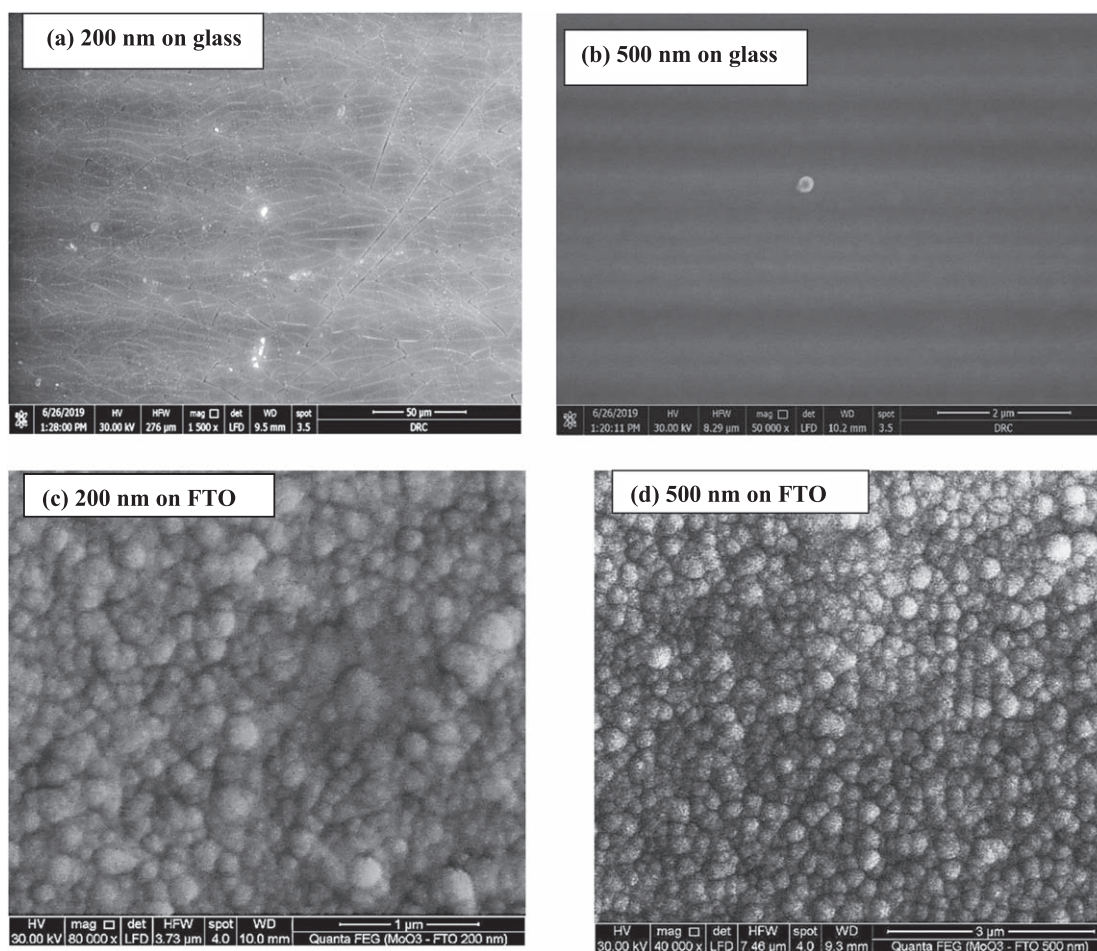


Figure 2. SEM micrographs of as deposited MoO_{3-x} thin films (a), (b) on glass with 200 and 500 nm thick, respectively; and (c), (d) on FTO 200, 500 nm thick, respectively.

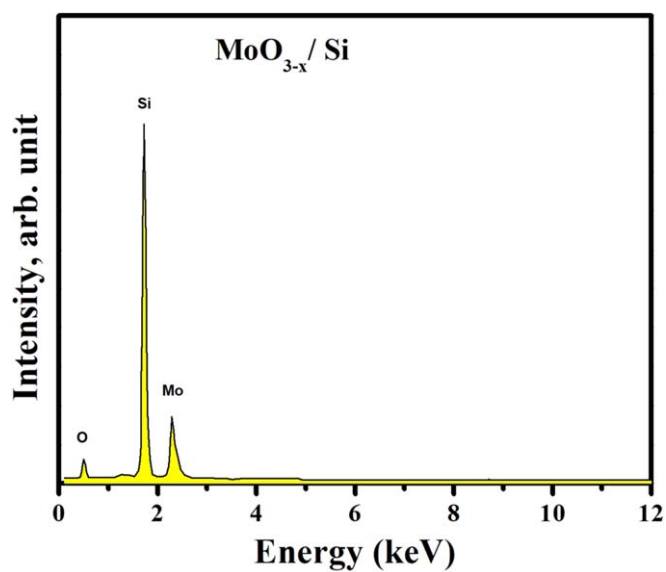


Figure 3. EDAX spectrum of as deposited MoO_{3-x} thin films on Si of 300 nm thick.

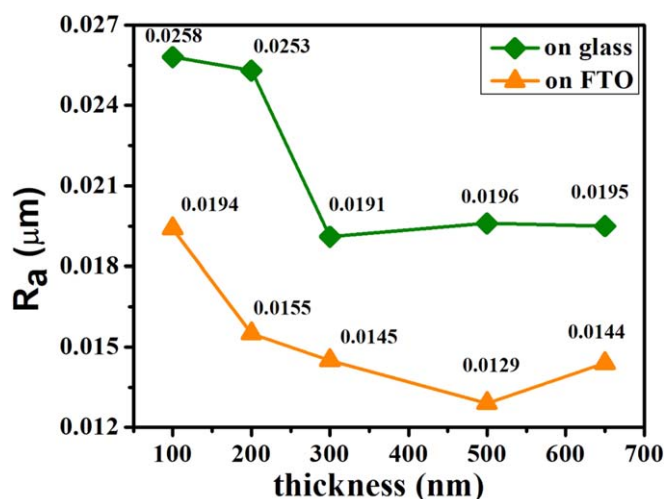


Figure 4. Variation of the Arithmetical mean roughness (R_a) with the film thickness for the as deposited MoO_{3-x} films on glass and FTO substrates.

the films deposited on FTO. It was found that MoO_{3-x} film deposited on glass with 300 nm thick has the lowest R_a value, whereas for MoO_{3-x} films deposited on FTO, the film with 500 nm thick has the lowest R_a value.

Figure 5 shows the optical transmittance and reflectance spectra of as deposited MoO_{3-x} films on glass and FTO coated glass. It is observed that the transmittance of MoO_{3-x} films either deposited on glass or FTO substrates decreases with increasing the film thickness in the spectral range from 460 to 970 nm. Degradation of the transparency confirms the presence of oxygen vacancies, which leads to the increase of the carrier concentration [22]. The color degree of films was observed to vary from nearly transparent to evident blue with increasing the film thickness. Besides, the observed shift in the absorption edge to longer wavelengths for MoO_{3-x} films either deposited on glass or FTO substrates indicates the decrease in the energy gap with increasing the film thickness.

As shown in figure 5(a), the transmittance of the deposited films on glass is very high in both visible (Vis) and near infrared regions (NIR). In contrast, MoO_{3-x} films deposited on FTO seemed to possess relatively weak transmission values in NIR region. This transmission is obviously annihilated as the wavelength increases (figure 5(b)). Such behavior of optical transmission of MoO_{3-x} films on FTO substrate may be due to the plasmonic reflection. On the other hand, no transmittance in the (UV) region was observed, indicating that at lower wavelengths, the incident light is absorbed.

The inset of figure 5 depicts the optical reflectance spectra of the as deposited MoO_{3-x} films on glass and FTO. The figures show that, the reflectance manifests an opposite behavior of transmittance. It can be seen also that, the reflectance of the deposited films on glass in the near infrared region (NIR) is less than that of the deposited films on FTO. The average values of reflectance for MoO_{3-x} films deposited on glass and FTO are 20 and 45%, respectively.

The behavior of reflectance of both films in the near infrared region (NIR) can be interpreted in terms of the concentration of charge carriers. The high reflectance in the NIR of MoO_{3-x} films deposited on FTO refers to the high carrier concentration.

Using the absolute values of the measured transmittance and reflectance with the film thickness ($d = 100, 200, 300, 500$ and 650 nm), the absorption coefficient (α) of the as deposited MoO_{3-x} films on glass and FTO was calculated according to the following relation [34]:

$$\alpha = \frac{1}{d} \ln \frac{(1 - R)^2}{T} \quad (2)$$

It was found that, all the observed α values for MoO_{3-x} films are corresponding to the high absorption region ($\alpha > 10^4 \text{ cm}^{-1}$).

The optical band gap of films was deduced using Tauc equation [28];

$$\alpha h\nu = \beta (h\nu - E_g)^n \quad (3)$$

where β is a constant, E_g is the optical band gap, n is a number that characterizes the type of electron transition where n is equal to 2 or 1/2 for allowed indirect or direct transitions, respectively and 3/2, 3 for forbidden direct and indirect transitions, respectively.

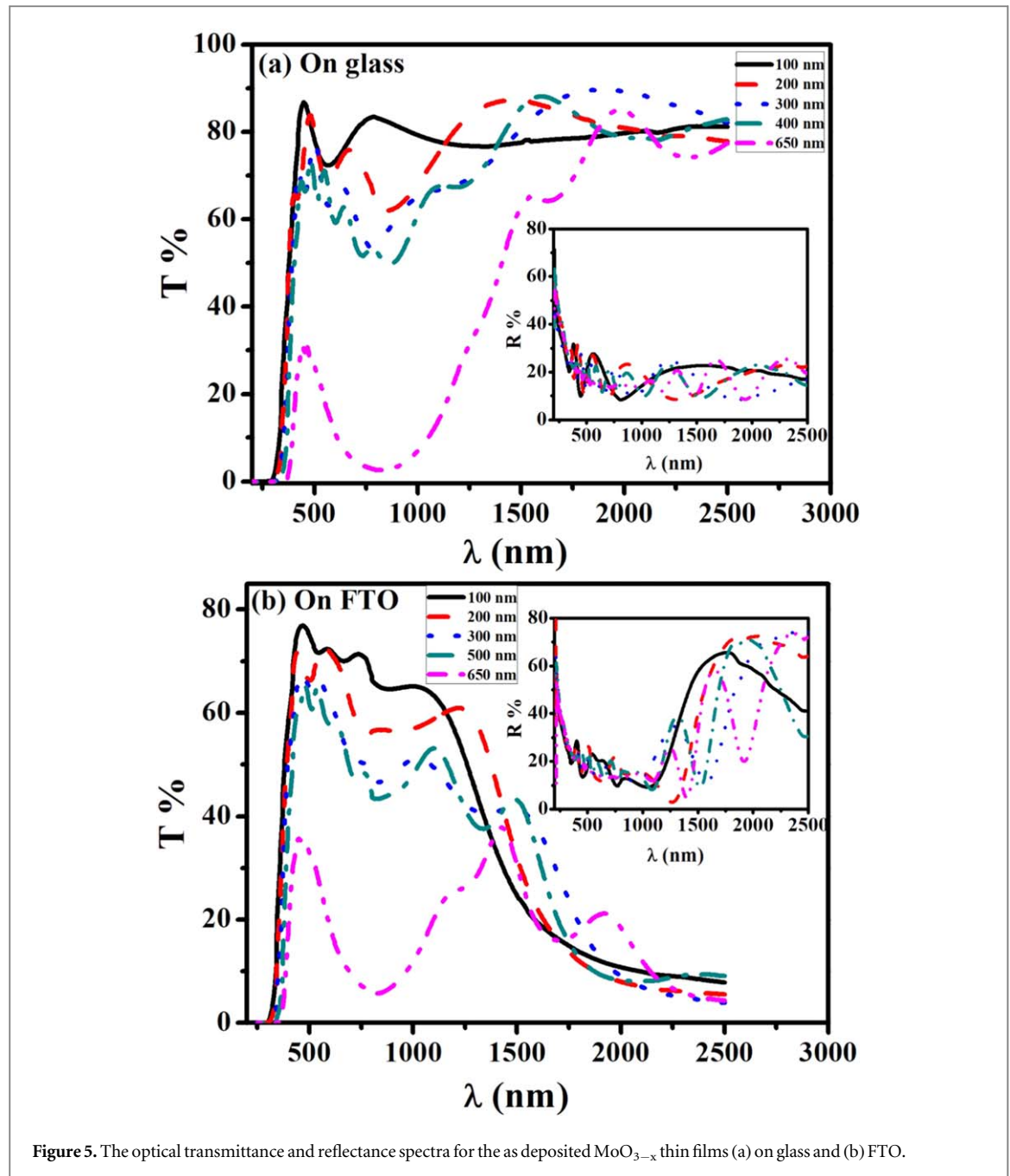


Figure 5. The optical transmittance and reflectance spectra for the as deposited MoO_{3-x} thin films (a) on glass and (b) FTO.

To confirm the transition type value, the following differentiation of equation (3), could be employed;

$$F(h\nu) = \frac{d(\ln \alpha h\nu)}{d(h\nu)} = \frac{n}{h\nu - E_g} \quad (4)$$

The equation indicates that $F(h\nu)$ tends to its maximum value as the photon energy ($h\nu$) approaches the energy gap E_g value.

$$\therefore [F(h\nu)]^{-1} = \left[\frac{d(\ln \alpha h\nu)}{d(h\nu)} \right]^{-1} = \frac{h\nu}{n} - \frac{E_g}{n} \quad (5)$$

Plotting the dependence of $[F(h\nu)]^{-1}$ versus $h\nu$ in the range of $\alpha > 10^4 \text{ cm}^{-1}$ should give a straight line. The slope of this line is equal to $(1/n)$. Values of n were illustrated in table 1.

Examination of our data reveals that, Tauc equation was satisfied for $n = 1/2$ that is corresponding to allowed direct transitions. The E_g values for MoO_{3-x} films deposited on glass and FTO coated glass substrates with thickness (100, 200, 300, 500 and 650 nm) were obtained also by extrapolating the linear portions of the plots of $(ah\nu)^2$ versus $h\nu$ to $\alpha = 0$ as shown in figure 6.

Table 1. The corresponding optical gap for MoO_{3-x} films deposited on glass and FTO coated glass, calculated by different two methods.

Thickness (nm)	Deposited films on glass				Deposited films on FTO			
	Slope = 1/n	Intercept	1/slope = n	E _g (eV)	Slope = 1/n	Intercept	1/slope = n	E _g (eV)
100	1.82	5.86	0.55	3.59	1.5	4.4	0.67	3.61
200	1.76	5.89	0.57	3.51	1.6	4.85	0.63	3.52
300	1.63	5.07	0.61	3.42	1.61	4.8	0.62	3.43
500	2.02	6.13	0.50	3.24	1.75	5.1	0.57	3.25
650	1.86	5.46	0.54	3.13	1.81	5.4	0.55	3.16

The corresponding optical energy gap (using equation (3)), E_g was illustrated in figure 6(c) and table 1. It's clear that the substrate type has no explicit effect on the optical band gap energy, since the measured transmittance data for both the MoO_{3-x} films deposited on glass and FTO have the same fundamental absorption edge.

For MoO_{3-x} films either deposited on glass or FTO, it was observed that, increasing the film thickness from 100 nm to 650 nm leads to the decrease of E_g from 3.6 to 3.13 eV which can be attributed to the shift of the absorption edge to lower energy. These E_g values of MoO_{3-x} films deposited on glass and FTO coated glass are in good agreement with results of other researchers [2, 19, 32].

The electrical resistivity (ρ) of MoO_{3-x} thin film was measured for film with 500 nm thick deposited on glass and FTO coated glass during the temperature decreasing regime from 575 to 300 K as depicted in figures 7(a), (b). The figure confirms the semiconductor behavior of MoO_{3-x} thin film. It is shown that, the electrical resistivity decreases gradually from 1.6×10^4 to $23.5 \Omega \text{ cm}$ for film deposited on glass; and from 5.3×10^{-3} to $1 \times 10^{-3} \Omega \text{ cm}$ for film deposited on FTO coated glass substrate with increasing the temperature. MoO_{3-x} film of 500 nm thick synthesized by the present method seemed to be colored suggesting it's containing a number of oxygen vacancies [4, 7] that act as donor centers.

Figure 8 depicts the temperature dependence of Seebeck coefficient, S-T relation, in the temperature range from 300 to 575 K. It's clear that Seebeck coefficient (S) has negative value in the relatively lower temperature range from 300 K to 425 K indicating that MoO_{3-x} thin film is n-type semiconductor, which may be due to the presence of extra metal Mo atoms [5]. Temperature elevating in air enhances the filling of oxygen vacancies and consequently the (n/p) ratio decreases leading to the decreases of electrons contribution in S- value. Zero value of S means a complete compensation between both contributions of electrons and holes.

Further elevating of the film temperature, Seebeck coefficient (S) start to be positive, referring to n- to p- type conduction behavior transition caused by the increase of the absorbed oxygen from air with film temperature rising. Positive S is achieved when the contribution of holes becomes more than that of electrons and continues up to $T \sim 485 \text{ K}$. Further elevation of temperature above 485 K seemed to be associated, beside the oxygen vacancies filling process, with Mo⁺ oxidation state formation by means of electron hopping from oxygen into metallic orbitals due to thermal ionization [2, 19, 35]. This leads to the increase of (n/p) ratio causing an improvement of electrons contribution in S. More temperature elevation makes the electrons contribution to be more important leading to the decrease of (+S) for $T > 485 \text{ K}$.

All present EDAX, optical and electrical measurements' confirms the presence of excess metal Mo atoms due oxygen deficiency, besides the films contains more Mo excess atoms. SEM and surface roughness measurements manifests the high compact and dense homogeneous surface of high thick MoO_{3-x} thin films deposited on glass and FTO, which makes the thick films can be used as a gas sensor material [22, 30, 36, 37].

Since, the sensing mechanism is based on the surface reaction of semiconducting oxide, whereas gases can be chemisorbed in air at the surface of the material [22], MoO_{3-x} film with 500 nm thick was tested optically for gas sensing applications.

Figure 9 shows the effect of chlorine exposure on the optical transmittance of MoO_{3-x} film with 500 nm thick deposited on glass and FTO coated glass substrates. The film transmittance was measured after different periods of exposure and at different concentrations of chlorine. The transmittance degrades as increasing the period of exposure to chlorine gas from 5 min to 107 min (figures 9(a), (c), indicating the sensitivity of MoO_{3-x} toward chlorine gas, where the absorption band edge was shifted towards longer wavelengths. Figure 10 shows the degradation of transmittance around $\lambda \approx 460 \text{ nm}$. It is clear that, T (%) decreases by increasing the exposure time and MoO_{3-x} films deposited on glass affected by Cl gas more than that deposited on FTO. We observed after 16 h of the last exposure time, the optical transmittance increased to be close to its initial value before chlorine exposure for the film deposited on glass, this reversible process suggests that MoO_{3-x} films grown on glass are promising in gas sensor applications. However, after the same period of the last gas exposure in the case of the film deposited on FTO substrate, the transmittance did not return to its original value before chlorine exposure. This may be due to the less deficiency of oxygen in MoO_{3-x} films deposited on FTO than that in film

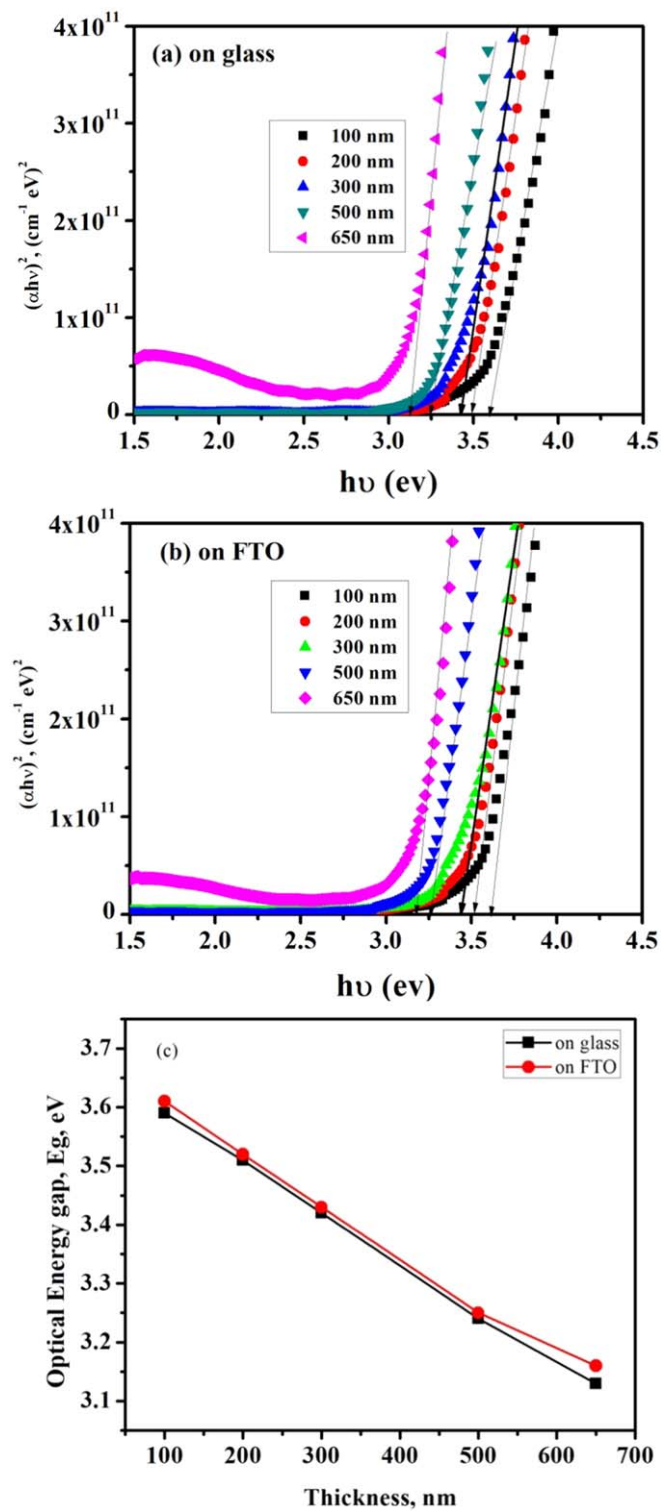


Figure 6. $(\alpha h\nu)^2$ versus $(h\nu)$ for MoO_{3-x} thin films with thickness (100,200,300,500 and 650 nm) (a) On glass, (b) On FTO and (c) The thickness dependence of optical energy gap.

deposited on glass. Increasing the concentration of chlorine gas at fixed exposure time for 10 min causing a slight change in (T%) for films deposited on glass and FTO substrates (figure (b), (d)).

To determine the best thickness that can be used as a high transparent conductive electrode for solar devices. Figure of Merit for MoO_{3-x} thin films deposited on FTO were calculated using the following relation;

$$\varphi_M = \frac{T}{\rho} \quad (6)$$

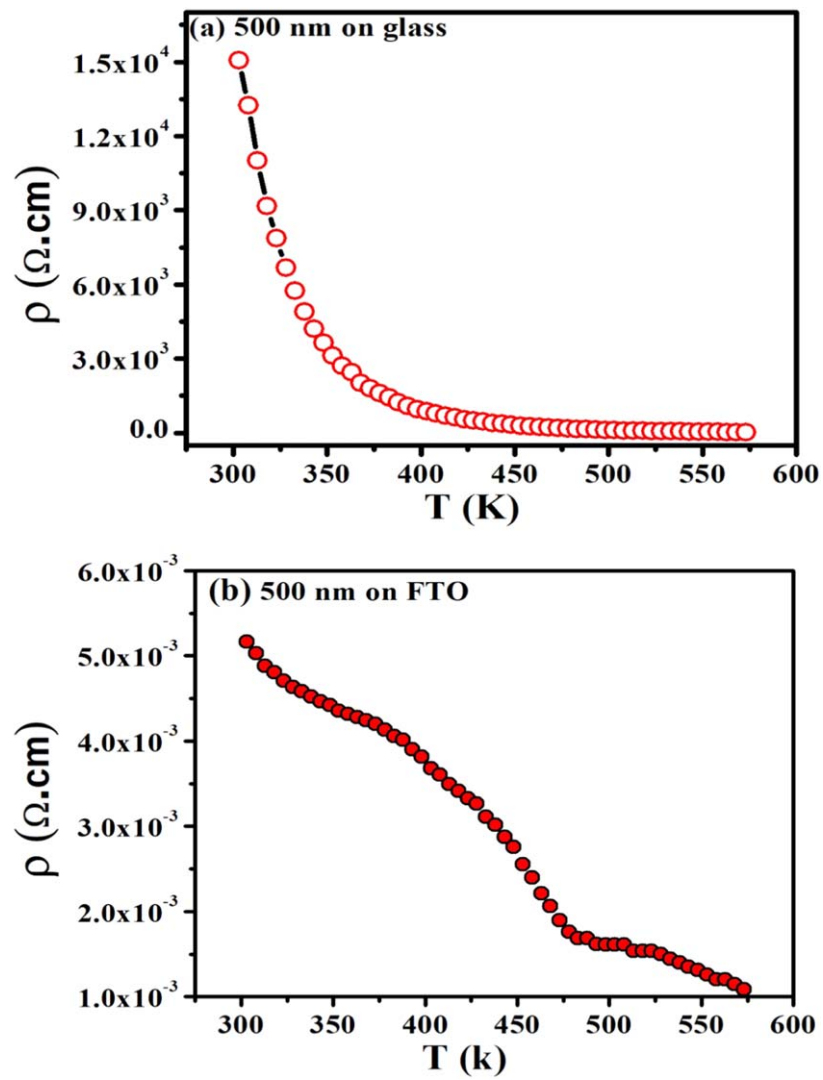


Figure 7. Temperature dependence of electrical resistivity for MoO_{3-x} film with 500 nm thick (a) deposited on glass and (b) on FTO coated glass substrates.

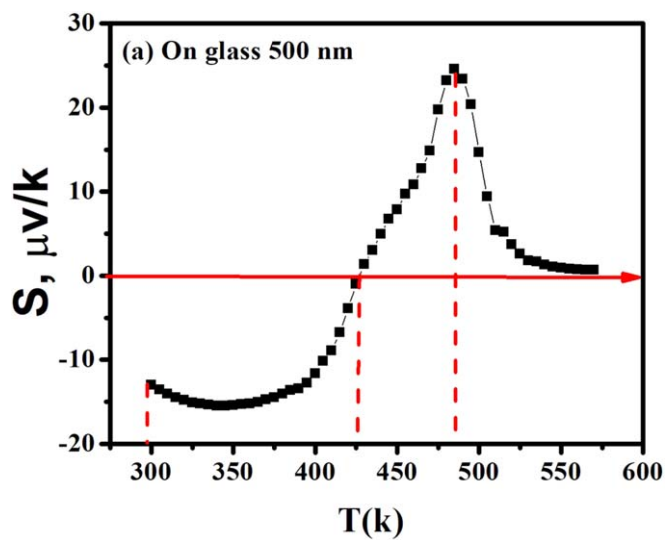


Figure 8. Seebeck coefficient versus the temperature change T (K) of MoO_{3-x} film with 500 nm thick on glass substrate.

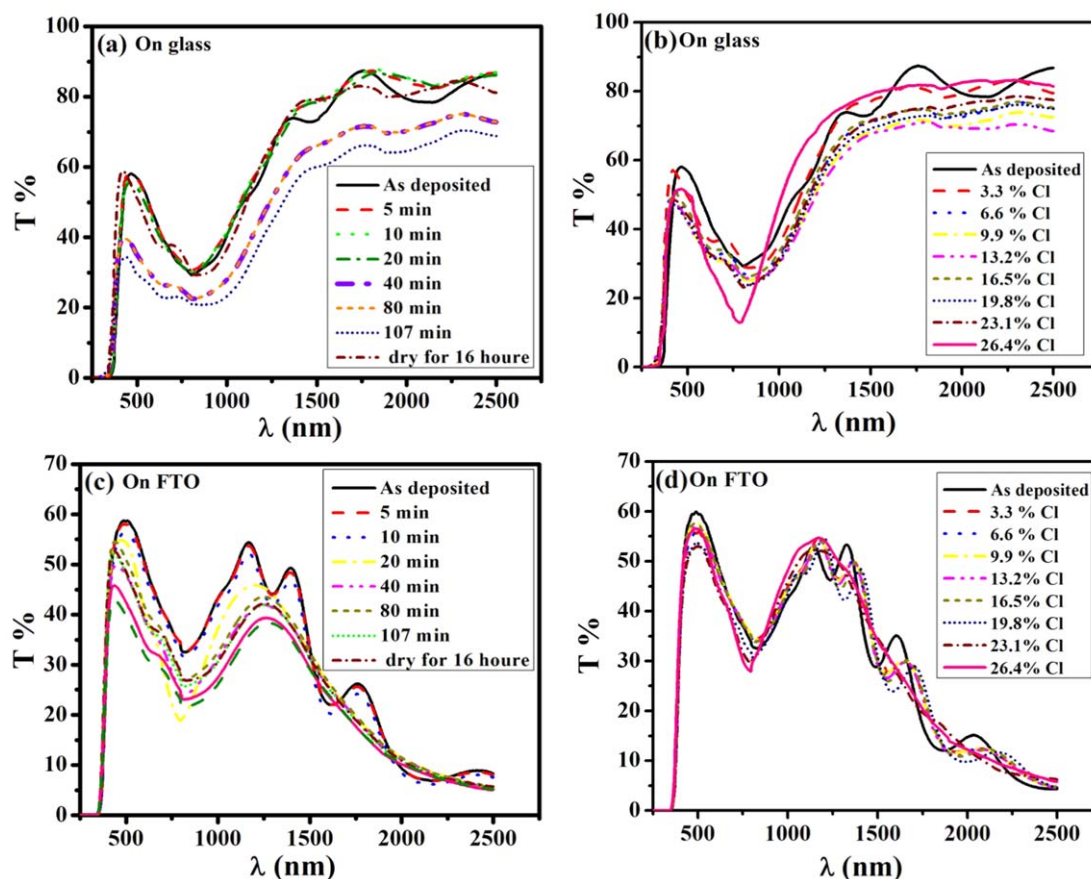


Figure 9. Chlorine exposure dependence of optical transmittance of MoO_{3-x} films deposited on glass and FTO.

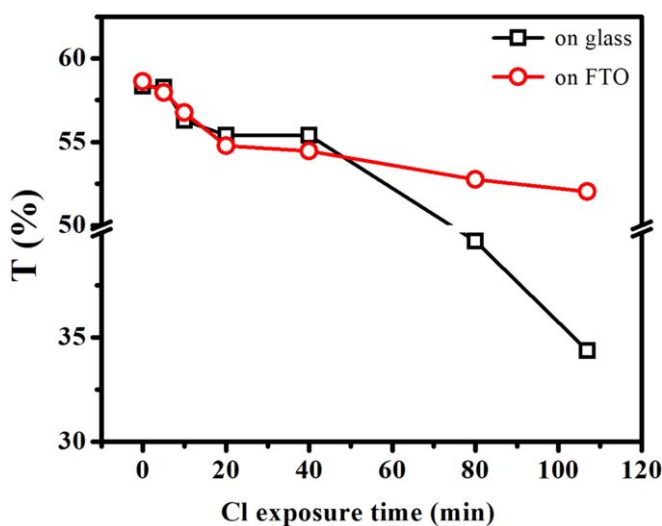


Figure 10. Transmittance degradation at wavelength 460 nm of MoO_{3-x} deposited on glass and FTO substrates.

were (T) is the optical transmittance in the visible range; (ρ) is the electrical resistivity of MoO_{3-x} thin films deposited on FTO at room temperature.

As depicts in figure 11, MoO_{3-x} thin film with 100 nm thick, deposited on FTO substrate has the highest figure of Merit value, which qualify it to be used as high conductive transparent electrodes for solar cell applications.

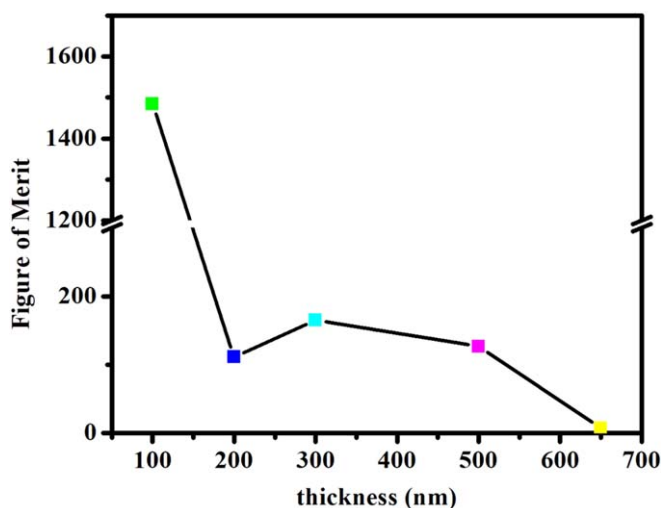


Figure 11. Figure of Merit of MoO_{3-x} thin films of 100, 200, 300, 500 and 650 nm thick deposited on FTO substrate.

4. Summary and conclusions

The structure investigation performed by x-ray diffraction shows that all the present MoO_{3-x} films are amorphous regardless the type of substrate. The chemical composition analysis carried out by EDAX shows a small MoO_{3-x} stoichiometry deviation indicating an excess of metallic Mo oxidation states acting as donor centers. SEM and surface roughness measurements manifests the high compact and dense homogeneous surface of MoO_{3-x} thin films deposited on glass and FTO, surface roughness of MoO_{3-x} films deposited on FTO were observed to be lower than those deposited on glass substrates. Transparency degradation of MoO_{3-x} films either deposited on glass or FTO substrates with increasing film thickness has been depicted. Besides, the reflection of these films was found to increases with increasing the wavelength, in NIR. Shifts of the absorption edge towards longer wavelengths are also observed with thickness, indicating that E_g —decreases from 3.6 to 3.13 eV. All these observations based on optical data confirm the increase of donor centers in films with film thickness increase.

MoO_{3-x} films of 500 nm thick were tested for using as a chlorine detection sensor. The observed transmittance was degraded with elongating the period of exposure showing the sensitivity of MoO_{3-x} to chlorine gas. For MoO_{3-x} film deposited on glass, it was found that, the chlorine gas adsorbed on the surface of the film and volatiles after a period of time, referring to the reversible gas sensor film and confirming that MoO_{3-x} films are promising in gas sensor applications.

The electrical resistivity measurements of MoO_{3-x} thin film of 500 nm thick deposited on glass and FTO coated glass substrates confirmed the semiconductor behavior of MoO_{3-x} thin film. Seebeck coefficient measurement showed the n- to p- type conduction behavior transition caused by the increase of absorbed oxygen from air. According to figure of Merit calculations of MoO_{3-x} deposited on FTO substrates, the high transmittance ($\sim 78\%$) in the visible spectral region besides the low resistivity ($\sim 10^{-3} \Omega \cdot \text{cm}$) of MoO_{3-x} film of 100 nm thick recommend it to be promising as a transparent conductive electrode for solar devices.

ORCID iDs

W S Mohamed  <https://orcid.org/0000-0003-4069-8637>

References

- [1] Kröger M, Hamwi S, Meyer J, Riedl T, Kowalsky W and Kahn A 2009 *Appl. Phys. Lett.* **95** 123301
- [2] Touihri S, Arfaoui A, Tarchouna Y, Labidi A, Amlouk M and Bernede J C 2017 *Appl. Surf. Sci.* **394** 414–24
- [3] Kim D Y, Subbiah J, Sarasqueta G, So F, Ding H, Irfan and Gao Y 2009 *Appl. Phys. Lett.* **95** 093304
- [4] Julien C, Mohammad Hussaxm O, E1-Farh L and Balkanski M 1992 *Solid State Ionics* 53–56, 400–4(North-Holland: SOLID STAT)
- [5] Peelaers H, Chabiniy M L and Van de Walle C G 2017 *Chem. Mater.* **29** 2563–7
- [6] Mizushima T, Moriya Y, Huu Huy Phuc N, Ohkita H and Kakuta N 2011 *Catal. Commun.* **13** 10–3
- [7] Khalate S A, Kate R S, Pathan H M and Deokate R J 2017 *J. Solid State Electrochem.* **21** 2737–46
- [8] Julien C and Nazri G A 1994 *Solid State Ionics* **68** 111–6
- [9] Phadungdhithidhad S, Mangkorntong P, Choopun S and Mangkorntong N 2008 *Ceram. Int.* **34** 1121–5
- [10] Lin S, Chen Y, Wang C, Hsieh P and Shih S 2009 *Appl. Surf. Sci.* **255** 3868–74
- [11] Boukhachem A, Kamoun O, Mrabet C, Mannai C, Zouaghi N, Yumak A, Boubaker K and Amlouk M 2015 *Mater. Res. Bull.* **72** 252–63

- [12] Shafieyan A R, Ranjbar M and Kameli P 2019 *Int. J. Hydrogen Energy* **44** 18628–38
- [13] Dai T, Ren y, Qian L and Liu X 2018 *J. Electron. Mater.* **47** 6709–6715
- [14] Wang G, Yang S, Dai J, Dai Y, Zou T, Roths J and Yang M 2019 *Sensors* **19** 4775
- [15] Wang M, Huang S, Zeng Y, Yang J, Pei J and Ruan S 2019 *Opt. Mater. Express* **9** 4429–37
- [16] Seo J, Moon Y, Lee S, Lee C, Kim D, Kim H and Kim Y 2019 *Nanoscale Horiz.* **4** 1221
- [17] Jin L, Zheng X, Liu W, Cao L, Cao Y, Yao T and Wei S 2017 *Journal of Materials Chemistry A* **5** 12022–12026
- [18] Boukhachem A, Bouzidi C, Boughalmi R, Ouerteni R, Kahlaoui M, Ouni B, Elhouichet H and Amlouk M 2014 *Ceram. Int.* **40** 13427–35
- [19] Sabhapathi V K, Md. Hussain O, Reddy P S, Reddy K T R, Uthanna S, Naidu B S and Redd P J 1995 *Phys. Stat. Sol. (a)* **148** 167
- [20] Nadkarni G S and Simmons J G 1970 *J. Appl. Phys.* **41** 545
- [21] Simmons J G 1967 *Phys. Rev.* **155** 657
- [22] Ali H M and Abdel Hakeem A M 2015 *Eur. Phys. J. Appl. Phys.* **72** 10301
- [23] Morales-Luna M, Tomas S A, Arvizu M A, Perez-Gonzalez M and Campos-Gonzalez E 2017 *J. Alloys Compd.* **722** 938–45
- [24] Tomás S A, Arvizu M A, Zelaya-Angel O and Rodríguez P 2009 *Journal of Thin Solid Films* **518** 1332–6
- [25] Mahajan S S, Mujawar S H, Shinde P S, Inamdar A I and Patil P S 2008 *Int. J. Electrochem. Sci.* **3** 953–60
- [26] Bogue R 2015 *Sensor Rev.* **35** 133–40
- [27] Liu X, Cheng S, Liu H, Hu S, Zhang D and Ning H 2012 *Sensors* **12** 9635–65
- [28] Tauc J, Grigorovici R and Vancu A 1966 *Physica Status Solid* **15** 627–37
- [29] Patil R S, Dplane M D and Patil P S *Appl. Surf. Sci.* **252** 8050–6
- [30] Ali H M and Abdel Hakeem A M 2010 *Phys. Status Solidi a* **207** 132–138
- [31] Mane A A and Moholkar A V 2017 *Appl. Surf. Sci.* **405** 427–40
- [32] Granqvist C G 2014 *Thin Solid Films* **564** 1–38
- [33] Zhang Z and Lagally M G 1997 *Science* **276**–5309 17–21
- [34] Ali H M, Shokr E K and Marchenko A V 2013 *Optoelectronics and Advanced Materials—Rapid Communications* **7** 207–13
- [35] Balaji M, Chandrasekaran J and Raja M 2016 *Mater. Sci. Semicond. Process.* **43** 104–13
- [36] Khojier K, Savaloni H and Zolghadr S 2014 *Appl. Surf. Sci.* **320** 315–21
- [37] Martí'nez H M, Torres J, Rodri'guez-Garci'a M E and Lo'pez Carren'ˆo L D 2012 *Physica B* **407** 3199–202